Results in Engineering 24 (2024) 102963

Contents lists available at ScienceDirect

Results in Engineering

journal homepage: www.sciencedirect.com/journal/results-in-engineering

Structural behavior of built-up I-shaped CFS beams

Ardalan B. Hussein [a,*], Diyari B. Hussein [b]

[a] Department of Structural Engineering and Geotechnics, Széchenyi István University, Egyetem Tér 1, 9026, Győr, Hungary
[b] Department of Architectural Engineering, Cihan University Sulaimaniya, Sulaimaniya, 46001, Iraq

ARTICLE INFO

Keywords:
Direct strength method (DSM)
Back-to-back channels
Buckling
Cold-formed steel (CFS)
Built-up I-Sections
Critical elastic buckling moment
Fastener spacing
Finite element analysis (FEA)
Flexural strength
Nominal elastic buckling moment
Screw spacing

ABSTRACT

The use of back-to-back built-up C-section beams is becoming increasingly common in CFS construction due to their cost-effectiveness and enhanced load-carrying capacity, making them suitable for longer beam spans and convenient for transportation. These built-up sections are utilized in wall studs, truss components, and floor joists, with intermediate screw fasteners placed at specific intervals to prevent the separate bowing of channels. This study reveals a ratio of 1.003 between experimental findings and finite element analysis results, and 1.002 between experimental findings and direct strength method results, indicating a strong correlation between experimental data from nonlinear finite element analysis and predictions based on the American Iron and Steel Institute and Australian and New Zealand Standards, particularly in predicting the flexural buckling strength of beam specimens. Furthermore, ongoing research is investigating the impact of screw spacing on flexural strength. This study presents results from 175 finite element tests, evaluating seven distinct cross-sections with twelve unique screw spacings. These spacings correspond to the half wavelength of local, distortional, and global buckling, divided by values from one to four. It was found that screw spacing based on half the local buckling half-wavelength along the centerline of the webs increased the critical global buckling moment capacity and the nominal flexural strength by 56 % and 27 %, respectively. For double-lane screws with the same spacing, these increases were even more substantial, reaching 65 % and 31 %, respectively. Economically, the recommended spacing for single-lane screws is half the local buckling half-wavelength.

1. Introduction

Cold-formed steel (CFS) sections present a number of significant advantages over conventional building materials. These include a high strength-to-weight ratio [1], which allows for efficient structural performance, and exceptional design flexibility, enabling a wide range of applications [2]. CFS also offers enhanced durability and fire resistance, contributing to safer and longer-lasting structures. Its lightweight [3–7] nature ensures ease of handling and transportation, while its precision manufacturing guarantees consistent quality and facilitates prefabrication. Furthermore, CFS is cost-effective [8,9], fully recyclable, and easily integrated with other materials, making it a versatile and sustainable option in modern construction.

This study focuses on the impact of screw configuration and spacing on the flexural capacity (moment resistance) of built-up cold-formed steel C-section beams. The goal is to optimize screw configurations to enhance the moment capacity of these beams. Common applications of CFS sections include their use in back-to-back configurations to form beam elements for steel trusses, space frames, and portal frames. In these configurations, intermediate screw fasteners are strategically placed along the length of the built-up sections to prevent individual sections from buckling independently.

Several types of fasteners are used to join CFS components, including screws, bolts, clinches, and spot welds [10]. Among these, screws can be employed to achieve a degree of composite action between elements, with optimal screw diameters ranging from 2.03 mm (0.08 in.) to 6.35 mm (0.25 in.) for steel-to-steel connections [11–13].

Moreover, minimum fastener edge distances are crucial for structural integrity. For instance, EUROCODE 3 prescribes a minimum distance from the end and edge equal to 1.2 times the bolt diameter [14]. However, for enhanced performance, the latest edition of AISI S100 mandates a more stringent minimum edge distance of 1.5 times the nominal screw or bolt diameter [12,13,15].

Furthermore, screw spacing significantly affects overall strength. Established design practices recommend limiting screw spacing to four times the web depth to minimize the risk of catastrophic collapse [16].

* Corresponding author.
E-mail addresses: hussein.ardalan.burhan@sze.hu (A.B. Hussein), diyari.burhan@sulicihan.edu.krd (D.B. Hussein).

https://doi.org/10.1016/j.rineng.2024.102963
Received 28 May 2024; Received in revised form 17 September 2024; Accepted 20 September 2024
Available online 21 September 2024

Research suggests that reducing the spacing between fasteners can lead to a higher ultimate capacity; however, this effect seems minimal when failure primarily stems from localized instabilities within individual components [17].

Optimal screw placement involves positioning them as close as possible to the joints between the flange and web [18]. Additionally, the flexural rigidity of screw-fastened built-up sections increases with the number of fastener rows, the number of fasteners per row, and particularly with the placement of additional fasteners towards the member's ends [10,19]. Connector spacing has a significant impact on eventual deflection [20]. To prevent a significant decrease in web strength due to excessive crippling, the ratio between the distance from the outer surface of the flange to the center of the screws and the overall web height of the built-up I-sections should not exceed 30 % [18].

Additionally, research indicates that the ability of screwed connections in CFS components to tilt and carry loads decreases as temperatures rise [21]. Built-up members present a design challenge due to partial composite action, where individual components do not fully act together. The extent of this interaction relies heavily on the shear stiffness of the connectors joining the parts. Notably, research has shown that spot and stitch welds provide a high degree of composite action [10].

In conclusion, by analyzing the influence of screw spacing and configuration, this investigation aims to provide valuable insights for optimizing the moment capacity of built-up cold-formed steel C-section beams.

2. Design standards for members without holes subject to bending

This study investigates the design of cold-formed steel (CFS) members for bending loads in the absence of holes. Established design codes, such as AISI S100 [11,12] and AS/NZS 4600 [22], provide explicit principles and criteria for these members. These principles consider factors like material properties, member geometry, bending stiffness, required strength, and overall structural behavior under bending. However, intermittent connections in back-to-back built-up beams create uneven cross-sections, making it difficult to determine the effective area using the effective width method (EWM) [23]. To address this challenge, this work explores the direct strength method (DSM) [11–13,15,24] as an alternative design approach for calculating the capacity of these back-to-back built-up CFS channel sections. Furthermore, this work proposes a method to convert critical linear elastic moments obtained from finite element analysis (FEM) to nominal linear elastic moments using the aforementioned design codes.

2.1. Global (lateral-torsional) buckling

For members susceptible to both yielding and global (lateral-torsional) buckling, the nominal flexural strength at first yield, M_{ne}, shall be computed using the following equation:

$$\mathbf{F}_{cre} = \frac{\mathbf{M}_{cre}}{\mathbf{S}_x} \quad (1)$$

$$\mathbf{M}_y = \mathbf{F}_y \times \mathbf{S}_f \quad (2)$$

$$M_{ne} = \mathbf{F}_n \times \mathbf{S}_{fc} \leq \mathbf{M}_y \quad (3)$$

$$\textit{if } \mathbf{F}_{cre} \geq \mathbf{2.78} \times \mathbf{F}_y, \textit{then } \mathbf{F}_n = \mathbf{F}_y \quad (4)$$

$$\textit{if } \mathbf{F}_{cre} \leq \mathbf{0.56} \times \mathbf{F}_y, \textit{then } \mathbf{F}_n = \mathbf{F}_{cre} \quad (5)$$

$$\textit{For } \mathbf{2.78} \times \mathbf{F}_y > \mathbf{F}_{cre} > \mathbf{0.56} \times \mathbf{F}_y, \textit{then } \mathbf{F}_n = \frac{\mathbf{10}}{\mathbf{9}} \times \mathbf{F}_y \times \left(\mathbf{1} - \frac{\mathbf{10} \times \mathbf{F}_y}{\mathbf{36} \times \mathbf{F}_{cre}}\right) \quad (6)$$

M_{ne} represents the nominal flexural strength concerning yielding and overall buckling, Mcre indicates the critical moment for elastic global buckling, while S_{fc} denotes the elastic section modulus of the entire unaltered section in relation to the extreme compression fiber. F_{cre} signifies the critical stress for elastic lateral-torsional buckling, whereas S_f indicates the elastic section modulus of the complete unaltered cross-section relative to the extreme fiber during initial yielding. F_y stands for the yield stress, and M_y represents the moment at which the member yields.

2.2. Local buckling

Each component must undergo assessment to ascertain any potential decrease in its available strength, referred to as factored resistance, resulting from the interplay between yielding or global buckling and local buckling. In accordance with the Direct Strength Method, the nominal flexural strength, denoted as $_{Mnl,}$ concerning local buckling, shall be established as follows:

$$\lambda_\ell = \sqrt{\overline{\mathbf{M}}_{ne} / \mathbf{M}_{crl}} \quad (7)$$

$$\textit{For } \lambda_\ell \leq 0.776, \textit{then } \mathbf{M}_{n\ell} = \mathbf{M}_{ne} \quad (8)$$

$$\textit{When } \lambda_\ell > 0.776, \mathbf{M}_{n\ell} = \left[\mathbf{1} - \mathbf{0.15} \times \left(\frac{\mathbf{M}_{cr\ell}}{\overline{\mathbf{M}}_{ne}}\right)^{0.4}\right] \times \left(\frac{\mathbf{M}_{cr\ell}}{\overline{\mathbf{M}}_{ne}}\right)^{0.4} \times \overline{\mathbf{M}}_{ne} \quad (9)$$

$$\overline{\mathbf{M}}_{ne} = \textit{Lesser of } M_{ne} \textit{ and } M_y \quad (10)$$

M_{ne} represents the nominal resistance to lateral-torsional flexural strength, M_y denotes the yield moment of the member, and M_{crl} indicates the critical moment for elastic local buckling.

2.3. Distortional buckling

The nominal flexural resistance (M_{nd}) related to distortional buckling must be determined following the guidelines provided in this section. These regulations are applicable to various types of open cross-section members, including but not limited to I-, Z-, C-sections with compression flanges equipped with edge stiffeners, as well as U-, Hat-, panel-, or similar cross-sections with compression flanges, or any cross-section featuring intermediate stiffeners subjected to compression.

$$\lambda_d = \sqrt{\mathbf{M}_y / \mathbf{M}_{crd}} \quad (11)$$

$$\textit{If } \lambda_d \leq \mathbf{0.673}, \textit{then } \mathbf{M}_{nd} = \mathbf{M}_y \quad (12)$$

$$\textit{When } \lambda_d > 0.673, \mathbf{M}_{nd} = \left[\mathbf{1} - \mathbf{0.22} \times \left(\frac{\mathbf{M}_{crd}}{\mathbf{M}_y}\right)^{0.5}\right] \times \left(\frac{\mathbf{M}_{crd}}{\mathbf{M}_y}\right)^{0.5} \times \mathbf{M}_y \quad (13)$$

$$\mathbf{M}_n = M_{DSM} = \textit{Minimum of } (\mathbf{M}_{ne}, \boldsymbol{M}_{n\ell}, \textit{and } \mathbf{M}_{nd}) \quad (14)$$

$$\phi_b = 0.90 \ (LRFD)$$

When M_{crd} is Critical elastic distortional buckling moment. Also, Minimum of them controls the member.

3. DSM and finite element model validation

The research employed six back-to-back built-up cold-formed steel (CFS) channels as beam members for validation purposes. Initially, the test specimens were manufactured from G550 cold-formed steel sheets using a press brake. Subsequently, the individual channel pieces were assembled in a back-to-back configuration with self-drilling screws. Specifically, three distinct screw spacings were investigated: 1900 mm, 950 mm, and 475 mm. Furthermore, the built-up parts were standardized to a length of 2000 mm. Key material properties included a Young's modulus of 204.4 GPa, a yield stress (Fy) of 555.2 MPa, and an ultimate stress (Fu) of 592.7 MPa. Measurements of all test specimens were meticulously documented in Table 1.

Additionally, K. Roy and colleagues [25] conducted four-point bending tests on all specimens using a hydraulic jack loading frame with a force capacity of 500 kN (see Fig. 1). The separation between the two loading sites was maintained at 600 mm. For support conditions, the beams were simply supported with the left side (BC1) having boundary conditions U1, U2, UR2, and UR3 set to zero, while the right side (BC2) had boundary conditions U1, U2, U3, UR2, and UR3 set to zero. During experimental testing, a wooden piece was inserted between the specimens and the loading point, which resulted in a friction coefficient of 0.5 being used in the Finite Element (FE) model. The tangential behavior between the back-to-back channels was modeled using frictionless contact, with no physical interaction or insertion between the contacting surfaces. This methodological approach ensured that the interactions were accurately represented in the model.

A displacement rate of 0.03 mm/s was applied to all beams under displacement-controlled loading conditions. Linear Variable Differential Transformers (LVDTs) were positioned along the centerline of the tension face of each specimen to measure vertical displacements, and additional LVDTs were placed along the web to monitor lateral displacements. A data acquisition system was employed to continuously record both the applied load and the corresponding displacement data throughout the testing process.

A nonlinear elasto-plastic finite element (FE) model was constructed utilizing ABAQUS finite element software to analyze the behavior of back-to-back built-up cold-formed steel (CFS) channel sections subjected to four-point bending. Specifically, CFS channel segments were represented by S4R shell elements. To achieve precise results, all specimens were characterized by a small mesh size of 4 mm × 4 mm. Furthermore, to simulate the interaction between single channel beams and the loading points on the upper flanges of the beams, a "surface to surface" contact approach was utilized. This method ensured an accurate representation of the physical interactions occurring during the loading process.

The flexural capacity of the back-to-back built-up cold-formed steel (CFS) channel section beams was validated through a two-pronged approach: finite element analysis (FEA) and direct strength method (DSM) analysis. To facilitate a comprehensive understanding, a detailed comparison of these methods is presented in Table 2. The results indicate a high level of agreement between experimental testing and computational simulations. Specifically, the average ratio of experimental moment capacity to FEA moment capacity (M_{EXP}/M_{FEA}) is 1.003, with a low standard deviation (S) of 0.017. This close agreement underscores the reliability of the FEA in predicting the performance of the beams.

Furthermore, the average ratio of experimental moment capacity to DSM moment capacity (M_{EXP}/M_{DSM}) is 1.002 with a standard deviation of 0.015. This similarity between the experimental results and DSM analysis further validates the accuracy of the DSM in assessing the flexural capacity of the beams. Additionally, the FEA and DSM results showed close agreement with each other, exhibiting an average FEA-to-DSM moment capacity ratio (M_{FEA}/M_{DSM}) of 0.999 and a standard deviation of 0.011. This close correlation between FEA and DSM results is noteworthy and reinforces the consistency between these two analytical methods.

Moreover, the observed failure modes provide further support for the validity of the computational models. The lateral-torsional buckling modes observed in the experimental specimens at ultimate load (Figs. 2 and 3) closely match those predicted by the FEA model. This congruence between observed and predicted failure modes highlights the robustness of the FEA approach. Finally, Fig. 4 presents a comparison of the moment versus displacement curves obtained from both experimental testing and FEA models, further solidifying the high level of agreement between these methods. This consistency across different evaluation techniques underscores the reliability and accuracy of the flexural capacity predictions for the back-to-back built-up CFS channel section beams.

4. Numerical study

4.1. General

This investigation assessed the performance of 175 simply supported beams, all constructed from back-to-back cold-formed steel (CFS) channel sections acting as built-up flexural members. To accurately model the behavior of these built-up sections, a linear elastic finite element (FE) model was generated using ABAQUS software. The beams, made from S355 steel with specific material properties including a yield stress of 355 MPa, density of 78.49047 × 10^{-10} g/mm^3, Young's modulus of 210 GPa, and Poisson's ratio of 0.3, were subjected to end moments. Seven distinct C-channel profiles were utilized in creating the built-up open sections, as illustrated in Fig. 5. The individual channels were connected in a back-to-back configuration using self-drilling screws with a consistent radius of 2.4 mm. Investigating two screw connection configurations – single and double horizontal lanes, as depicted in Fig. 5– the study explored a total of twelve distinct screw spacings, with corresponding measurements and details provided in Table 3. The built-up sections were uniformly designed with a fixed length of 5000 mm, and the specific dimensions of each test specimen are outlined in Fig. 5.

4.2. Specimen labeling

To facilitate unambiguous identification, each built-up beam specimen was assigned a nomenclature reflecting its key dimensional characteristics. These characteristics include web depth (D), flange width (B), lip length (d), and inner bent radius (Ri). As shown in Figs. 5 and 6, these designated dimensions are visually represented for clarity.

For example, the designation "2C200 × 75 × 20 × 2.5″ can be deconstructed as follows. Firstly, "2C″ denotes the utilization of two Cold Formed steel C-sections arranged in a back-to-back configuration. Secondly, "200″ corresponds to the web depth, designated as D = 200 mm (mm). Thirdly, "75″ represents the flange width, designated as B = 75 mm. Additionally, "20″ indicates the lip length, designated as d = 20 mm. Finally, "2.5″ specifies the thickness of the sections, designated as t = 2.5 mm. It is noteworthy that all dimensions are expressed in millimeters, and the inner bent radius (Ri) is consistently maintained at twice

Table 1
Dimensions of the beam specimens [25].

Beam ID	Web Depth	Flange Length	Thickness	Internal radius	Lip Length	Screw Spacing	Section Modulus
	D	B	t	Ri	d	S	S_x
	mm						mm^3
BU90-S1900	90.2	50.7	1.22	1.5	14.5	1895.3	7645
BU90-S1900-R	91.6	50.9	1.2	1.5	14.8	1904.5	7717
BU90-S950	89.5	50.2	1.18	1.49	15.7	955.6	7344
BU90-S950-R	89.8	49.7	1.19	1.48	15.9	947.5	7392
BU90-S475	90.4	50.4	1.2	1.5	15.4	472.8	7563
BU90-S475-R	90.9	50.6	1.21	1.52	14.6	476.3	7656

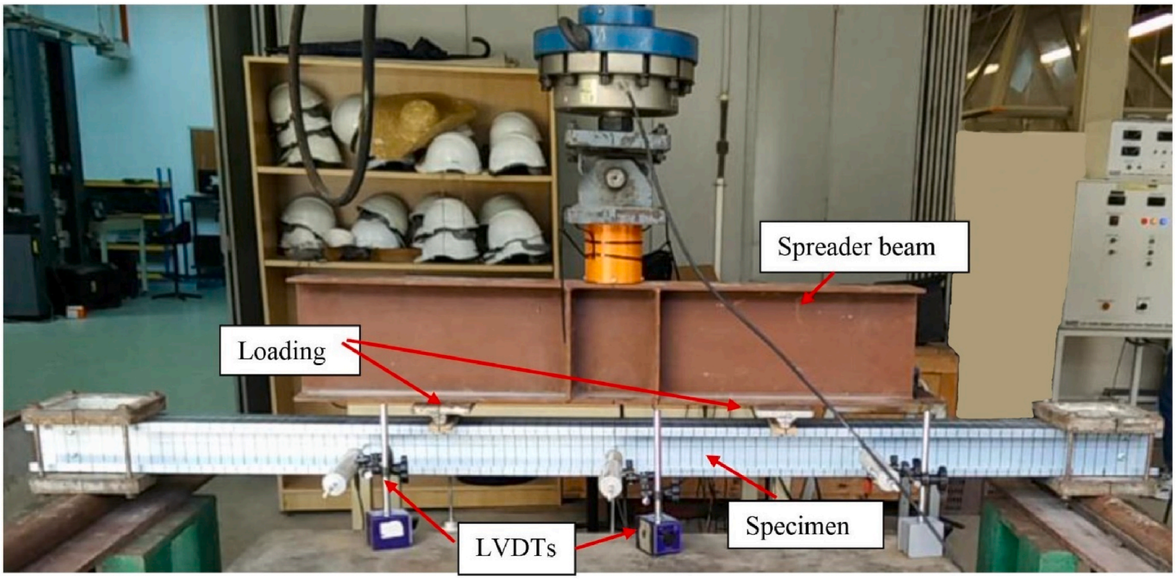

Fig. 1. Experimental setup for four-point bending test of back-to-back built-up CFS channel beams [25].

Table 2
Experimental results compared with FEA and DSM findings.

Beam ID	M_{EXP}	M_{FEA}	M_{DSM}	M_{EXP}/ M_{FEA}	M_{EXP}/ M_{DSM}	M_{FEA}/ M_{DSM}
	kN. m	kN. m	kN.m	-	-	-
BU90-S1900	4.57	4.66	4.64	0.98	0.98	1.00
BU90-S1900-R	4.46	4.44	4.42	1.00	1.01	1.00
BU90-S950	4.81	4.75	4.71	1.01	1.02	1.01
BU90-S950-R	4.87	4.88	4.86	1.00	1.00	1.00
BU90-S475	4.99	4.84	4.94	1.03	1.01	0.98
BU90-S475-R	4.94	4.97	5.02	0.99	0.98	0.99
Mean				1.003	1.002	0.999
S				0.017	0.015	0.011

the member's thickness.

4.3. Dimensions of beam specimens

This investigation delves into the influence of critical geometric parameters on the bending moment capacity of built-up open channels constructed from back-to-back C-sections (Fig. 5). Specifically, the study employs a meticulously designed approach involving seven distinct C-section profiles, each enabling the isolation and variation of a specific dimension. To isolate the effect of web depth, the research systematically alters this parameter between 100 mm, 150 mm, and 200 mm, while holding all other dimensions (flange width, lip length, thickness, inner radius, and beam length) constant. Furthermore, similar controlled comparisons are conducted by varying flange width (50 mm, 65 mm, and 75 mm) and section thickness (1.5 mm, 2.0 mm, and 2.5 mm), with all other parameters remaining unchanged. This rigorous approach, by isolating key factors, aims to establish a comprehensive understanding of how targeted geometric modifications influence the bending performance of built-up cold-formed steel (CFS) beams. Consequently, the findings from this study are expected to provide valuable insights into optimizing the design of such structures.

4.4. Screw arrangements

Within this investigation, seven distinct cross-sectional channels were interconnected in a back-to-back configuration through the utilization of screws. Conforming to the stipulations outlined in the AISI S100 standards [11,12], the screws employed possessed a radius falling within the range of 1.015 mm–3.175 mm, with the specific radius in this study being set at 2.4 mm. As delineated in Fig. 6, two discrete screw configurations were implemented. The initial configuration involved a single lane of screws situated along the centerline of the webs to effectuate the interconnection of the back-to-back channels. Conversely, the alternative configuration employed two horizontal lanes of screws for this purpose. Notably, in the latter configuration, the vertical distance from the centerline of the top screw lane to the upper surface of the top flange measured 20 mm, mirroring the distance from the centerline of the bottom screw lane to the lower surface of the bottom flange. Moreover, in both the single-lane and double-lane screw arrangements, a uniform horizontal distance of 20 mm from the center of the first and last screws to the initiation or termination point of the built-up beams was maintained.

4.5. Exploring screw spacing

This study undertook a rigorous examination of screw spacing's influence on structural behavior. A comprehensive investigation was conducted, encompassing twelve discrete screw spacings, each applied to configurations featuring single and double screw lanes. The precise screw spacings for all test specimens have been meticulously cataloged in Table 3 for reference. Noteworthy among these designations is "0S," which signifies configurations where no screws are employed to connect back-to-back channels. Furthermore, the parameters "Lg," "Ld," and "Ll" signify the half-wavelengths of critical elastic global, distortional, and local buckling, respectively, as determined by the CUFSM [26] tool, with all measurements expressed in millimeters. It is a sophisticated engineering software tailored for the analysis of thin-walled steel sections, enabled accurate determination of these critical parameters. Additionally, by dividing each half-wavelength by factors of one, two, three, and four, a spectrum of twelve distinct screw spacings for channel connection was derived, ultimately leading to the creation of 175 models within the ABAQUS Finite Element Software.

Transitioning to the assessment of structural integrity, Mcrl, Mcrd, Mcre, and Mn represent the critical elastic local, distortional, global, and

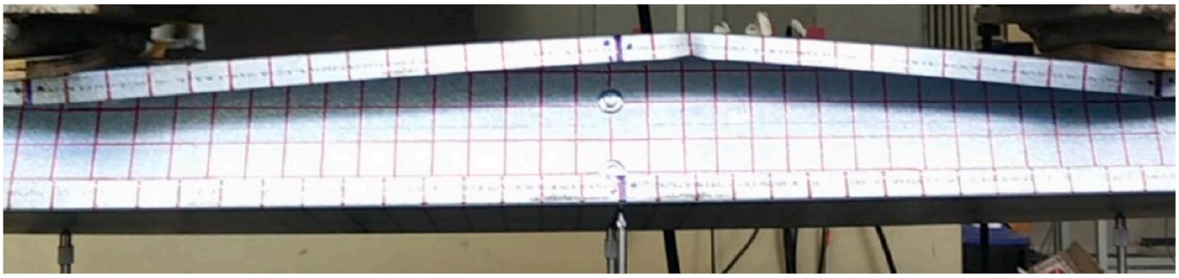

(a). Experiment [22]

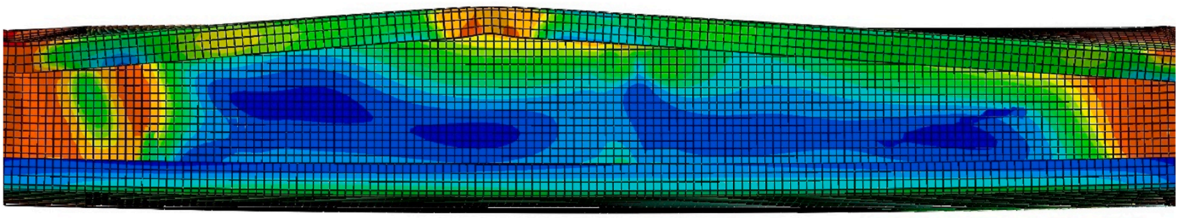

(b). FEM

Fig. 2. Failure mode of back-to-back assembled CFS channel beam BU90-S950.

(a). Experiment [22]

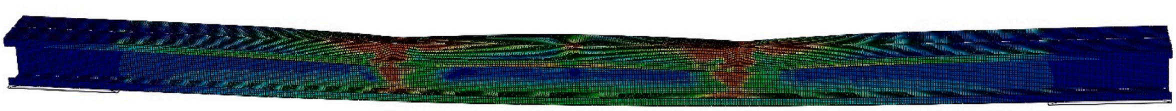

(b). FEM

Fig. 3. Failure mode of back-to-back assembled CFS channel beam BU90-S475.

nominal buckling moments, respectively. These pivotal values, measured in kN × m, were ascertained under conditions where no screws were employed to connect back-to-back single channels, serving as essential benchmarks for comparative analysis (see Table 3).

4.6. *Finite element meshing and end boundary conditions*

The FE beam specimens in this study were constructed using ABAQUS [27] through the implementation of 3D deformable shell elements. This choice was motivated by the computational efficiency of shell sections, which offer faster processing times compared to solid sections. Subsequently, two reference points, denoted as RP-1 and RP-2, were affixed to both ends of the specimens, facilitating structural analysis. Through the application of a "Coupling Constraint," both ends of the specimens were firmly anchored to these reference points, as depicted in Fig. 7. Regarding boundary conditions, RP-1 was restricted from movement in the X and Y directions, as well as from rotation about the Z-axis, while RP-2 was constrained from movement in all three spatial dimensions and rotation about the Z-axis. To ascertain three distinct types of critical elastic local bending moments, negative and positive eigenvalue moments were respectively applied at RP-1 and RP-2. The analytical procedure entailed employing buckle linear perturbation with 200 eigenvalues.

Furthermore, the utilization of screws to join back-to-back open channels necessitated specific contact behaviors: "Frictionless" tangential behavior and "Hard Contact" normal behavior, facilitating subsequent separation of the channels. Mesh size in FE software significantly influences buckling result accuracy, with finer meshes enhancing precision. Thus, a mesh size of 5 mm × 5 mm, employing S4R element types [28–30], was selected to ensure the reliability of the study's outcomes.

5. Numerical analysis and results

In this section, elastic linear analyses were used to determine the moment capacity of back-to-back built-up CFS channel section beams. Elastic linear analysis is employed to find the buckling moment of thin-walled steel sections, and this analysis is divided into two different procedures. The older procedure is the effective width method (EWM), while the newer and more accurate procedure is the direct strength method (DSM). In this study, the new procedure (DSM) is used to determine the flexural strength of built-up back-to-back CFS channels.

The goal of this study is to find the best screw spacing to achieve

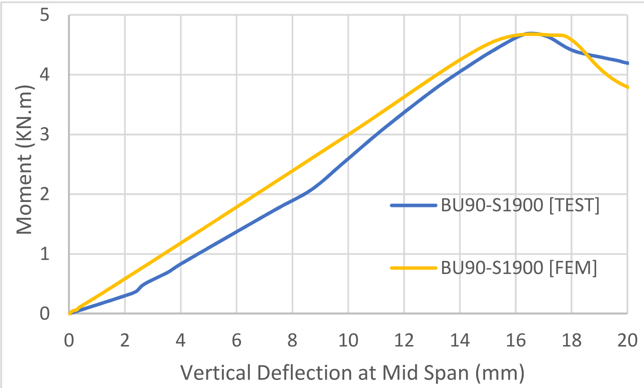

(a)- BU90-S1900

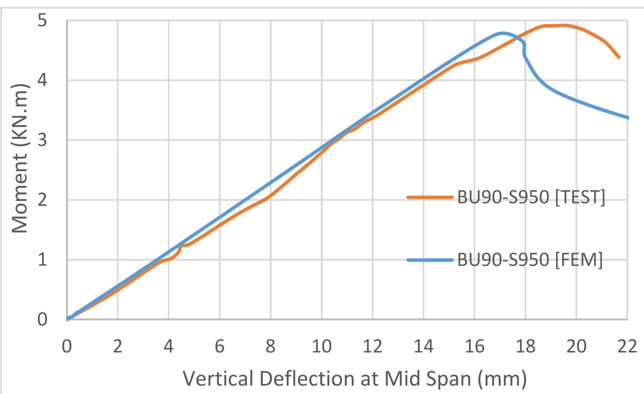

(a)- BU90-S950

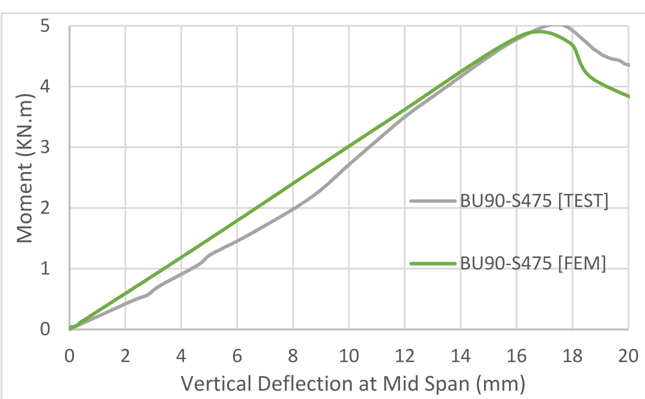

(a)- BU90-S475

Fig. 4. Graphs depicting the relationship between moment and vertical displacement.

optimal critical elastic local, distortional, and global buckling moments, as well as to determine the optimal nominal buckling moment of built-up CFS channels.

First, three different types of critical moments were found through finite element analysis software, ABAQUS. These three types of moments consist of critical elastic local (M_{crl}), distortional (M_{crd}), and global (M_{cre}) buckling moments. Next, using the equations provided in SECTION 2, these three types of buckling moments are converted into three different types of nominal buckling moments: nominal elastic local (M_{nl}), distortional (M_{nd}), and global (M_{ne}) buckling moments. Subsequently, by choosing the minimum of the nominal moments and multiplying by 0.90, the available flexural strength (ϕ_b M_n) is obtained.

In this study, symbols have been introduced to simplify the representation of various built-up sections. The symbol (A) represents section 2C200 × 75 × 20 × 2.5, while (B) denotes 2C200 × 75 × 20 × 2. The symbol (C) is used for 2C200 × 75 × 20 × 1.5, and (D) represents section 2C150 × 75 × 20 × 2. For section 2C150 × 65 × 20 × 2, the symbol (E) is used, and (F) corresponds to 2C150 × 50 × 20 × 2. section 2C100 × 75 × 20 × 2 is indicated by the symbol (G). Additionally, the symbol (Av.) denotes the average of all sections in Table 3, Table 4, Table 5, Tables 6, and Table 7, the symbol "I" indicates the use of one lane of screws, whereas "II" signifies the use of two lanes of screws to connect back-to-back CFS channels.

An analysis of Table 4 reveals that employing a single lane of screws exerts a minimal influence on the critical elastic local buckling moment (M_{crl}). Conversely, utilizing two lanes of screws demonstrably impacts M_{crl}. On average, with screw spacings of Ll/2, Ll/3, and Ll/4, Mcrl increases by 7 %, 8 %, and 9 %, respectively, for a single lane of screws. Notably, this effect intensifies to 14 %, 18 %, and 20 % for two lanes of screws, respectively.

Intriguingly, the influence of screw spacing on both single lane (I) and double lane (II) configurations remains relatively constant when solely the section thickness varies. This consistency persists as long as other parameters, such as web depth, flange width, lip length, bend radius, and beam length, are held constant. However, a pronounced increase in the impact of screw spacing is observed for both screw lane configurations when only the flange width is reduced while other dimensions remain unchanged.

An examination of Table 5 reveals a negligible effect from employing a single lane of screws on the critical elastic distortional buckling moment (M_{crd}). In contrast, utilizing two lanes of screws demonstrably impacts M_{crd}. Notably, a positive correlation exists between decreasing screw spacing and increasing M_{crd} when two lanes of screws connect built-up CFS channels. Specifically, M_{crd} increases by 11 %, 15 %, 16 %, and 17 %, respectively, for screw spacings of Ll/1, Ll/2, Ll/3, and Ll/4, when two lanes of screws are employed.

Furthermore, consistent with the observations for M_{crd}, the influence of screw spacing on both single lane (I) and double lane (II) configurations remains relatively constant under two specific scenarios. First, this consistency persists when only the section thickness varies, and second, it holds true when only the flange width changes. As long as other parameters, such as web depth, lip length, bend radius, and beam length, are held constant, this trend is maintained.

In summary, the data indicates that the configuration and spacing of screws play a significant role in determining the buckling moments, especially in the case of double lane configurations. The variations in screw spacing and the consequent impact on M_{crd} highlight the importance of precise screw placement in optimizing the structural performance of built-up CFS channels.

As shown in Table 6, using one lane of screws and two lanes of screws generally has a major impact on the critical elastic global buckling moment (M_{cre}). Notably, even using three screws (Lg/2) to connect single channels together can increase M_{cre} by approximately 37 %.

On the other hand, the impact of screw spacing for both one lane and two lanes of screws remains approximately unchanged under specific conditions. This stability is observed when only the thickness of the section changes while other dimensions remain constant, when only the flange width of a section changes while other dimensions are stable, and when only the web depth of a section changes with other dimensions held constant.

In general, as depicted in Table 7 and Fig. 8, the utilization of one lane of screws and two lanes of screws exerts a significant influence on the nominal elastic global buckling moment (M_n). Remarkably, even the implementation of three screws (Lg/2) to connect built-up back-to-back single channels results in an approximate 20 % increase in M_n for both types of screw lanes.

Interestingly, the impact of screw spacing for both single-lane and double-lane screw configurations remains relatively stable under

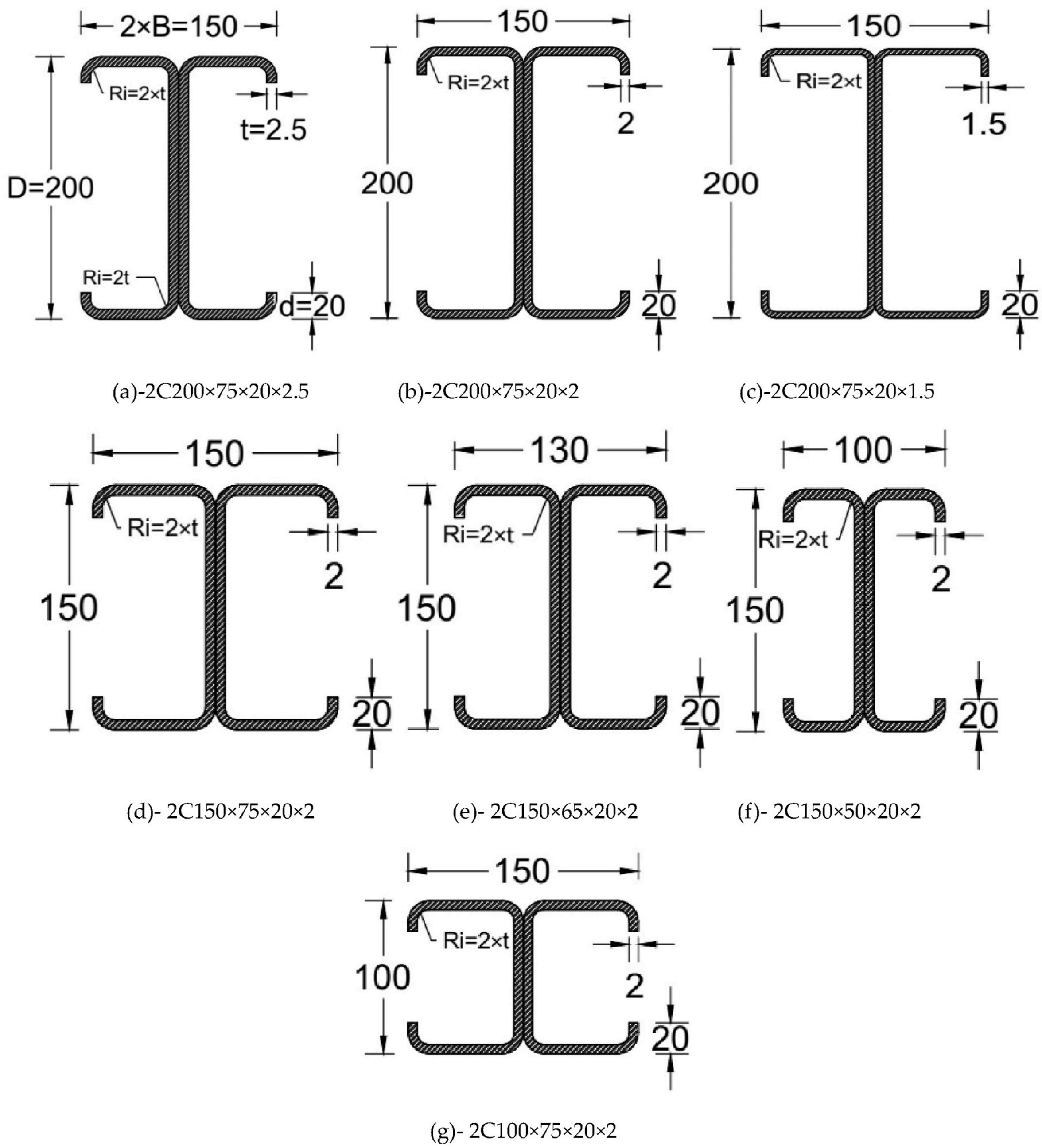

Fig. 5. Cross-sectional dimensions of beam specimens.

specific circumstances. This stability is evident when only the thickness of the section changes while other dimensions remain constant, as well as when only the web depth of a section changes while other dimensions remain stable.

In light of the presented analyses, it is recommended to optimize the available flexural strength (ϕ_b M_n) of built-up back-to-back channel specimens. To achieve an optimal balance between maximizing M_n and economic considerations, employing at least three screws (Lg/2) is recommended. This configuration demonstrably enhances ϕ_b M_n and offers a robust solution for applications demanding superior flexural strength.

6. Conclusion

This study extensively examined the flexural behavior of back-to-back cold-formed steel (CFS) channel section beams connected with screws through a comprehensive finite element analysis (FEA) of 175 models. Seven distinct channel cross-sections and various screw connection configurations were analyzed, with a focus on local, distortional, and global buckling modes. Validation of the FE model was achieved through a rigorous comparison with experimental test results, which confirmed its accuracy in predicting failure modes and flexural capacities. The consistency of experimental-to-FEA and direct strength method (DSM) results further affirmed the reliability of the model, with average ratios of experimental moment capacity to FEA and DSM moment capacities being 1.003 and 1.002, respectively.

A notable finding of this research is the significant impact of screw spacing on the flexural capacity of the beams, particularly for slender configurations. Optimal screw spacing, specifically at half the local buckling half-wavelength for single-lane screws, resulted in increased critical elastic local buckling moment, critical elastic distortional buckling moment, critical elastic global buckling moment, and nominal

Table 3
Number of screws in each row for built-up beams and critical and nominal moments for specimens with zero screws.

ID	2C200 × 75 × 20 × 2.5 (A)	2C200 × 75 × 20 × 2 (B)	2C200 × 75 × 20 × 1.5 (C)	2C150 × 75 × 20 × 2 (D)	2C150 × 65 × 20 × 2 (E)	2C150 × 50 × 20 × 2 (F)	**2C100 × 75 × 20 × 2 (G)**	**Average (Av.)**
	Number of screws per line							
0S	–	–	–	–	–	–	–	–
Lg/1	2	2	2	2	2	2	2	2
Lg/2	3	3	3	3	3	3	3	3
Lg/3	4	4	4	4	4	4	4	4
Lg/4	5	5	5	5	5	5	5	5
Ld/1	10	9	8	9	10	12	10	10
Ld/2	19	17	15	18	20	24	18	19
Ld/3	29	25	22	26	29	35	27	28
Ld/4	38	33	28	34	38	46	35	36
Ll/1	45	46	47	66	64	61	74	58
Ll/2	88	91	92	132	127	122	147	114
Ll/3	132	136	138	197	189	182	220	171
Ll/4	175	181	183	262	252	243	293	227
Moment (kN × m)								
Mcrl (0S)	102	52	22	46	52	53	29	51
Mcrd (0S)	63	40	22	32	35	41	22	36
Mcre (0S)	28	22	17	16	12	7	11	16
Mn(0S)	25	22	15	15	12	7	10	15

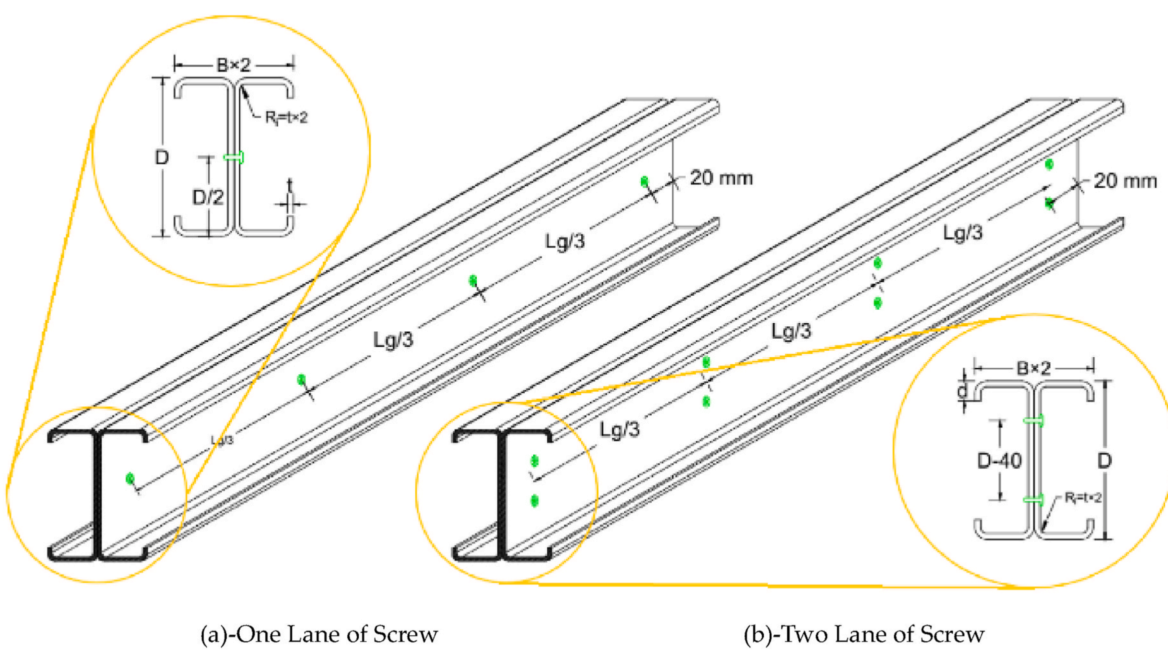

Fig. 6. Screw arrangement for the connection of back-to-back channel beams.

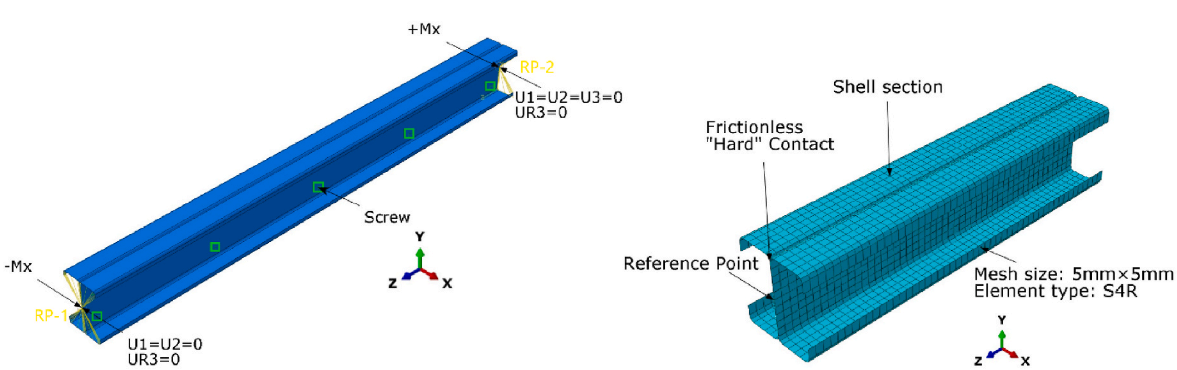

Fig. 7. Boundary conditions (left) and mesh properties (right) for shell finite element modeling.

Table 4
Ratio of critical elastic local buckling moment for a built-up section with screws to that without screws ($M_{crl}/M_{crl}(0S)$).

ID	(A)		(B)		(C)		(D)		(E)		(F)		(G)		(Av.)	
	I	II	I	II	I	II	I	II	I	II	I	II	I	II	I	II
0S	1.00	1.00	1.00	1.00	1.00	1.00	1.00	1.00	1.00	1.00	1.00	1.00	1.00	1.00	1.00	1.00
Lg/1	1.00	1.00	1.00	1.00	1.00	1.00	1.00	1.00	1.00	1.00	1.00	1.00	1.00	1.00	1.00	1.00
Lg/2	1.00	1.00	1.00	1.00	1.00	1.00	1.00	1.00	1.00	1.00	1.00	1.00	1.00	1.00	1.00	1.00
Lg/3	1.00	1.00	1.00	1.00	1.00	1.00	1.00	1.00	1.00	1.00	1.00	1.00	1.00	1.00	1.00	1.00
Lg/4	1.00	1.00	1.00	1.00	1.00	1.00	1.00	1.00	1.00	1.00	1.00	1.00	1.00	1.00	1.00	1.00
Ld/1	1.00	1.01	1.00	1.01	1.00	1.00	1.00	1.00	1.00	1.00	1.00	1.01	1.00	1.00	1.00	1.00
Ld/2	1.01	1.02	1.01	1.02	1.01	1.01	1.00	1.00	1.00	1.01	1.01	1.03	1.00	1.00	1.01	1.01
Ld/3	1.01	1.03	1.00	1.01	1.00	1.01	1.00	1.00	1.00	1.01	1.00	1.02	1.00	1.00	1.00	1.01
Ld/4	1.03	1.06	1.03	1.05	1.01	1.03	1.00	1.00	1.01	1.02	1.04	1.07	1.00	1.00	1.02	1.03
Ll/1	1.03	1.06	1.04	1.07	1.04	1.07	1.01	1.02	1.02	1.06	1.04	1.12	1.00	1.00	1.03	1.06
Ll/2	1.09	1.17	1.09	1.18	1.09	1.18	1.02	1.06	1.05	1.11	1.12	1.26	1.01	1.03	1.07	1.14
Ll/3	1.11	1.22	1.12	1.23	1.12	1.23	1.02	1.07	1.06	1.13	1.16	1.34	1.01	1.03	1.08	1.18
Ll/4	1.12	1.25	1.13	1.26	1.13	1.25	1.02	1.07	1.06	1.14	1.17	1.38	1.01	1.04	1.09	1.20

Table 5
Ratio of Critical Elastic Distortional Buckling Moment for a Built-Up Section with Screws to the Same member without Screws ($M_{crd}/M_{crd}(0S)$).

ID	(A)		(B)		(C)		(D)		(E)		(F)		(G)		(Av.)	
	I	II	I	II	I	II	I	II	I	II	I	II	I	II	I	II
0S	1.00	1.00	1.00	1.00	1.00	1.00	1.00	1.00	1.00	1.00	1.00	1.00	1.00	1.00	1.00	1.00
Lg/1	1.00	1.00	1.00	1.00	1.00	1.00	1.00	1.00	1.00	1.00	1.00	1.00	1.00	1.00	1.00	1.00
Lg/2	1.00	1.00	1.00	1.00	1.00	1.00	1.00	1.00	1.00	1.01	1.00	1.00	1.00	1.00	1.00	1.00
Lg/3	1.00	1.00	1.00	1.01	1.00	1.00	1.00	1.00	1.00	1.00	1.00	1.00	1.00	1.00	1.00	1.00
Lg/4	1.00	1.01	1.00	1.00	1.00	1.00	1.00	1.00	1.00	1.01	1.00	1.00	1.00	1.01	1.00	1.00
Ld/1	1.00	1.01	1.00	1.01	1.00	1.00	1.01	1.01	1.00	1.01	1.00	1.02	1.02	1.02	1.00	1.01
Ld/2	1.01	1.05	1.01	1.05	1.00	1.02	1.01	1.04	1.01	1.04	1.01	1.06	1.03	1.04	1.01	1.04
Ld/3	1.01	1.08	1.01	1.07	1.00	1.00	1.01	1.05	1.01	1.06	1.02	1.09	1.03	1.05	1.01	1.06
Ld/4	1.02	1.10	1.01	1.09	1.00	1.02	1.02	1.07	1.02	1.08	1.02	1.11	1.03	1.06	1.02	1.08
Ll/1	1.02	1.11	1.02	1.12	1.02	1.12	1.02	1.11	1.02	1.12	1.03	1.13	1.03	1.09	1.02	1.11
Ll/2	1.02	1.15	1.02	1.16	1.02	1.16	1.02	1.14	1.02	1.15	1.03	1.18	1.04	1.12	1.03	1.15
Ll/3	1.03	1.16	1.02	1.17	1.02	1.18	1.02	1.15	1.03	1.15	1.04	1.19	1.04	1.12	1.03	1.16
Ll/4	1.03	1.17	1.02	1.18	1.02	1.18	1.02	1.15	1.03	1.16	1.04	1.19	1.04	1.13	1.03	1.17

Table 6
Ratio of critical elastic global buckling moment of built-up channels with screws to built-up section without screws ($M_{cre}/M_{cre}(0S)$).

ID	(A)		(B)		(C)		(D)		(E)		(F)		(G)		(Av.)	
	I	II	I	II	I	II	I	II	I	II	I	II	I	II	I	II
0S	1.00	1.00	1.00	1.00	1.00	1.00	1.00	1.00	1.00	1.00	1.00	1.00	1.00	1.00	1.00	1.00
Lg/1	1.00	1.00	1.00	1.00	1.00	1.00	1.00	1.00	1.00	1.00	1.00	1.00	1.00	1.00	1.00	1.00
Lg/2	1.37	1.37	1.38	1.38	1.30	1.35	1.42	1.42	1.38	1.39	1.33	1.33	1.44	1.44	1.37	1.38
Lg/3	1.42	1.45	1.44	1.47	1.29	1.30	1.50	1.53	1.46	1.48	1.40	1.42	1.55	1.57	1.44	1.46
Lg/4	1.45	1.48	1.46	1.49	1.29	1.34	1.53	1.56	1.49	1.51	1.42	1.44	1.59	1.62	1.46	1.49
Ld/1	1.48	1.52	1.49	1.53	1.30	1.29	1.57	1.60	1.53	1.56	1.46	1.49	1.64	1.67	1.50	1.52
Ld/2	1.50	1.55	1.51	1.56	1.32	1.33	1.59	1.63	1.54	1.59	1.47	1.53	1.66	1.69	1.51	1.55
Ld/3	1.50	1.57	1.52	1.57	1.31	1.31	1.60	1.64	1.55	1.60	1.47	1.55	1.67	1.70	1.52	1.56
Ld/4	1.51	1.59	1.52	1.58	1.31	1.33	1.60	1.65	1.55	1.61	1.47	1.56	1.67	1.71	1.52	1.58
Ll/1	1.51	1.59	1.53	1.59	1.52	1.55	1.60	1.68	1.55	1.63	1.47	1.58	1.68	1.74	1.55	1.62
Ll/2	1.51	1.61	1.53	1.61	1.54	1.61	1.61	1.69	1.56	1.65	1.48	1.60	1.68	1.76	1.56	1.65
Ll/3	1.51	1.62	1.53	1.62	1.54	1.61	1.61	1.69	1.56	1.65	1.48	1.61	1.68	1.76	1.56	1.65
Ll/4	1.51	1.62	1.53	1.62	1.54	1.62	1.61	1.70	1.56	1.66	1.48	1.61	1.68	1.77	1.56	1.66

flexural strength by 7 %, 3 %, 56 %, and 27 %, respectively. For double-lane screws with equivalent spacing, these improvements were even more pronounced, with increases of 14 %, 15 %, 65 %, and 31 %, respectively.

Comparison of the FEA results with established standards (AISI and AS/NZS) demonstrated strong correlation, particularly in predicting flexural buckling strength. These findings highlight the critical role of screw spacing in optimizing the flexural capacity of built-up I-shaped CFS beams. The insights gained from this study provide a valuable framework for researchers and engineers in the CFS field, offering a reliable basis for predicting the flexural capabilities of back-to-back built-up CFS channel section beams. Economically, setting the screw spacing to half the local buckling half-wavelength for single-lane screws is recommended to ensure efficient and structurally sound design.

CRediT authorship contribution statement

Ardalan B. Hussein: Writing – review & editing, Writing – original draft, Validation, Supervision, Software, Methodology, Investigation, Funding acquisition, Formal analysis, Conceptualization. **Diyari B. Hussein:** Visualization, Resources, Data curation.

Declaration of competing interest

The authors declare the following financial interests/personal relationships which may be considered as potential competing interests:

Table 7
Ratio of nominal elastic buckling moment of a built-up section with screws to the same member without screws ($M_n/M_n(0S)$).

ID	(A)		(B)		(C)		(D)		(E)		(F)		(G)		(Av.)	
	I	II	I	II	I	II	I	II	I	II	I	II	I	II	I	II
0S	1.00	1.00	1.00	1.00	1.00	1.00	1.00	1.00	1.00	1.00	1.00	1.00	1.00	1.00	1.00	1.00
Lg/1	1.00	1.00	1.00	1.00	1.00	1.00	1.00	1.00	1.00	1.00	1.00	1.00	1.00	1.00	1.00	1.00
Lg/2	1.18	1.18	1.19	1.19	1.10	1.12	1.18	1.18	1.25	1.25	1.33	1.33	1.16	1.16	1.20	1.20
Lg/3	1.20	1.21	1.21	1.21	1.10	1.11	1.20	1.21	1.29	1.30	1.40	1.42	1.18	1.19	1.23	1.23
Lg/4	1.21	1.22	1.21	1.22	1.10	1.11	1.21	1.22	1.30	1.31	1.42	1.44	1.19	1.20	1.23	1.25
Ld/1	1.22	1.23	1.22	1.23	1.11	1.10	1.22	1.23	1.31	1.33	1.46	1.49	1.20	1.21	1.25	1.26
Ld/2	1.22	1.24	1.23	1.24	1.11	1.12	1.23	1.24	1.32	1.34	1.47	1.53	1.21	1.21	1.25	1.27
Ld/3	1.22	1.24	1.23	1.25	1.11	1.11	1.23	1.24	1.32	1.34	1.47	1.55	1.21	1.21	1.26	1.28
Ld/4	1.22	1.25	1.23	1.25	1.11	1.12	1.23	1.24	1.32	1.35	1.47	1.56	1.21	1.22	1.26	1.28
Ll/1	1.23	1.25	1.23	1.25	1.17	1.18	1.23	1.25	1.32	1.35	1.47	1.57	1.21	1.22	1.27	1.30
Ll/2	1.23	1.25	1.23	1.26	1.19	1.23	1.23	1.25	1.33	1.36	1.48	1.59	1.21	1.22	1.27	1.31
Ll/3	1.23	1.26	1.23	1.26	1.20	1.25	1.23	1.25	1.33	1.36	1.48	1.59	1.21	1.22	1.27	1.31
Ll/4	1.23	1.26	1.23	1.26	1.20	1.26	1.23	1.25	1.33	1.36	1.48	1.60	1.21	1.22	1.27	1.32

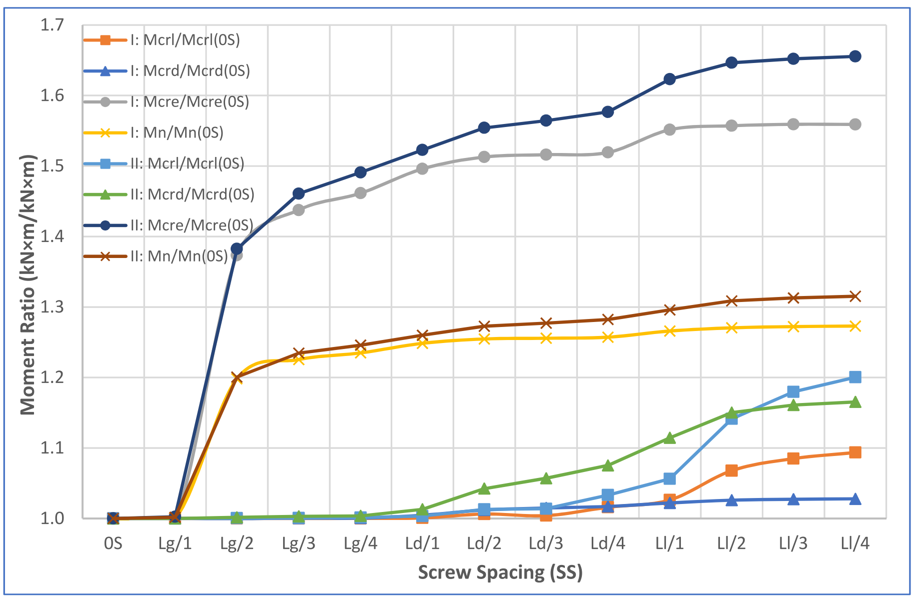

Fig. 8. Correlation between bending moment and screw spacing.

Ardalan B. Hussein reports financial support was provided by Széchenyi István University. Ardalan B. Hussein reports a relationship with Széchenyi István University Doctoral School of Multidisciplinary Engineering Sciences that includes:. If there are other authors, they declare that they have no known competing financial interests or personal relationships that could have appeared to influence the work reported in this paper.

Data availability

Data will be made available on request.

References

[1] M.A. Dar, S.J. Fayaz, S. Rather, A.R. Dar, I. Hajirasouliha, Incremental stiffening approach for CFS built-up-beams with large imperfections: tests and flexural-behaviour, Structures 53 (Jul. 2023) 1318–1340, https://doi.org/10.1016/j.istruc.2023.05.003.

[2] C. Liu, L. Duan, Analytical prediction of the distortional buckling loads for cold-formed Channel Beams with edge-stiffened rectangular web openings, Buildings 13 (1) (Jan. 2023), https://doi.org/10.3390/buildings13010101.

[3] J. Ye, S.M. Mojtabaei, I. Hajirasouliha, P. Shepherd, K. Pilakoutas, Strength and deflection behaviour of cold-formed steel back-to-back channels, Eng. Struct. 177 (Dec. 2018) 641–654, https://doi.org/10.1016/j.engstruct.2018.09.064.

[4] X. Zhao, W. Ma, W. Aiyiti, A. Kasimu, R. Jia, Investigation of influence of printing modes on the quality of 6-PSS FDM 3D printed thin-walled parts, Results in Engineering 17 (Mar) (2023), https://doi.org/10.1016/j.rineng.2023.100926.

[5] Q. Al-Kaseasbeh, Analysis of hydrocarbon fire-exposed cold-formed steel columns, Results in Engineering 20 (Dec. 2023), https://doi.org/10.1016/j.rineng.2023.101400.

[6] S. Senapati, K.K. Sangle, Nonlinear static analysis of cold-formed steel frame with rigid connections, Results in Engineering 15 (Sep) (2022), https://doi.org/10.1016/j.rineng.2022.100503.

[7] X. Yao, et al., Experiment and design of cold-formed steel equal-leg lipped angle under axial compression, Results in Engineering 23 (Sep) (2024), https://doi.org/10.1016/j.rineng.2024.102716.

[8] P. Keerthan, M. Mahendran, Improved shear design rules of cold-formed steel beams, Eng. Struct. 99 (Sep. 2015) 603–615, https://doi.org/10.1016/j.engstruct.2015.04.027.

[9] Q. Al-Kaseasbeh, Investigating the fire resistance of corrugated steel columns, Results in Engineering 21 (Mar) (2024), https://doi.org/10.1016/j.rineng.2023.101687.

[10] K.J.R. Rasmussen, M. Khezri, B.W. Schafer, H. Zhang, The mechanics of built-up cold-formed steel members, Thin-Walled Struct. 154 (Sep) (2020), https://doi.org/10.1016/j.tws.2020.106756.

[11] AISI, AISI S100-16 (R2020) w/S3-22 3 (2016) [Online]. Available: https://www.buildusingsteel.org/wp-content/uploads/2023/06/AISI-S100-16-2020-wS3-22.pdf. (Accessed 22 August 2024).

[12] AISI, AISI S100-16 (2020) w/S2-20 2 (2016) [Online]. Available: https://www.buildusingsteel.org/wp-content/uploads/2023/06/AISI-S100-16-2020-wS2-20.pdf. (Accessed 22 August 2024).

[13] Wei-Wen Yu, Roger A. LaBoube, Helen Chen, Cold-Formed Steel Design, fifth ed., John Wiley & Sons, 2020, 5th ed. https://www.wiley.com/en-us/Cold-Formed+Steel+Design%2C+5th+Edition-p-9781119487395. (Accessed 22 August 2024).

[14] E.N. Eurocode, 1993-1-8: Eurocode 3: Design of Steel Structures - Part 1-8: Design of Joints, John Wiley & Sons, 2005.

[15] AISI, AISI, 2020. S240-20.

[16] L. Wang, B. Young, Behaviour and design of cold-formed steel built-up section beams with different screw arrangements, Thin-Walled Struct. 131 (Oct. 2018) 16–32, https://doi.org/10.1016/j.tws.2018.06.022.
[17] F.J. Meza, J. Becque, I. Hajirasouliha, Experimental study of cold-formed steel built-up beams, J. Struct. Eng. 146 (7) (Jul. 2020), https://doi.org/10.1061/(asce)st.1943-541x.0002677.
[18] J. He, B. Young, Web crippling design of cold-formed steel built-up I-sections, Eng. Struct. 252 (Feb) (2022), https://doi.org/10.1016/j.engstruct.2021.113731.
[19] D.K. Phan, K.J.R. Rasmussen, Flexural rigidity of cold-formed steel built-up members, Thin-Walled Struct. 140 (Jul. 2019) 438–449, https://doi.org/10.1016/j.tws.2019.03.051.
[20] F. Portioli, G. Di Lorenzo, R. Landolfo, and F. Mazzolani, "CONTACT BUCKLING EFFECTS IN BUILT-UP COLD-FORMED STEEL BEAMS.".
[21] S.T. Vy, M. Mahendran, Screwed connections in built-up cold-formed steel members at ambient and elevated temperatures, J. Constr. Steel Res. 192 (May 2022), https://doi.org/10.1016/j.jcsr.2022.107218.
[22] AS/NZS, AS/NZS 4600: 2018 [Online]. Available: www.standards.govt.nz, 2018.
[23] D. Dubina, V. Ungureanu, R. Landolfo, Eurocode 3: Part 1-3, first ed., ECCS – European Convention for Constructional Steelwork, 2012 [Online]. Available: www.steelconstruct.com.
[24] AISI D100-08, American Iron and Steel Institute, 2008 [Online]. Available:.
[25] K. Roy, H. Ho Lau, T.C.H. Ting, B. Chen, J.B.P. Lim, Flexural behaviour of back-to-back built-up cold-formed steel channel beams: experiments and finite element modelling, Structures 29 (Feb. 2021) 235–253, https://doi.org/10.1016/j.istruc.2020.10.052.
[26] B.W. Schafer, S. Ádány, Buckling analysis of cold-formed steel members using CUFSM: conventional and constrained finite strip methods, in: *18th International Specialty Conference On Cold-Formed Steel Structures*, Orlando, Florida, 2006. Accessed: Sep. 09, 2024. [Online]. Available: www.ce.jhu.edu/bschafer/cufsm.
[27] Dassault Systèmes, Abaqus [Online]. Available: https://www.3ds.com/products/simulia/abaqus, 2024. (Accessed 18 August 2024).
[28] Cristopher D. Moen, B.W. Schafer, Direct strength design of cold-formed steel members with perforations [Online]. Available: https://scholarsmine.mst.edu/ccfss-aisi-spec/34/?utm_source=scholarsmine.mst.edu%2Fccfss-aisi-spec%2F34&utm_medium=PDF&utm_campaign=PDFCoverPages, Mar. 2009. (Accessed 9 September 2024).
[29] Z. yao Kim Jr rasmussen, Finite element modelling and Parametric studies of Perforated thin-Walled steel columns [Online]. Available: http://sydney.edu.au/civil, 2014.
[30] A. Mutafi, et al., An in-depth comparative FEA on through-thickness residual stresses in press-braked cold-formed steel section, Results in Engineering 22 (Jun) (2024), https://doi.org/10.1016/j.rineng.2024.102124.